Pilot scale concentration of cheese whey by forward osmosis: a short-cut method for evaluating the effective pressure driving force

Anna Artemi[1], George Q. Chen[2], Sandra E. Kentish[2], Judy Lee[1]*

[1]Department of Chemical and Process Engineering, University of Surrey, Guildford GU2 7XH, United Kingdom

[2] The ARC Dairy Innovation Hub, Department of Chemical Engineering, The University of Melbourne, Parkville, Victoria 3010, Australia

Key words: forward osmosis, pilot scale, whey concentration, osmotic pressure, concentration polarisation

*Corresponding Author:

Dr Judy Lee

Tel: +44 (0) 1483 682618

E-mail address: j.y.lee@surrey.ac.uk

Abstract

Cheese whey was concentrated to a concentration factor of 2.7 in a pilot scale forward osmosis filtration system, using a commercial cellulose triacetate membrane in a spiral-wound configuration. The whey was concentrated in a batch mode, using sodium chloride as the draw solution at initial osmotic pressures of 53 to 75 bar. During the process, flux was shown to reduce due to the simultaneous decrease in the bulk osmotic pressure of the draw solution, increase in the bulk osmotic pressure of the whey and the effect of concentration polarisation on both sides of the membrane. The flux is known to be driven by the effective osmotic pressures of whey and the draw solution on the surface of the membrane active layer. A short-cut approach that requires minimal information in advance about the osmotic pressure of whey and the geometry of the filtration system was implemented, enabling the determination of these effective osmotic pressures. The results obtained were shown to be in agreement with the fundamental forward osmosis flux model. The short-cut approach can be utilised for estimating effective osmotic pressures of other liquid food streams to be concentrated by forward osmosis, without the need of external measurements.

1 Introduction

Whey, the liquid remaining after curd formation in cheese making, is a valuable resource for the production of powders of high nutritional value [1]. Such a process requires the dehydration and drying of whey, which are usually achieved by thermal evaporation and spray drying, respectively. Evaporation is applied to increase the total solids content of whey to 40-70% [2,3] before drying to 95% or higher. Membrane filtration, mainly ultrafiltration and nanofiltration have been implemented for the separation of whey constituents and as a concentration step prior to thermal treatment, in order to reduce the total energy requirements for powder production [4]. When no separation of individual components is required, whey is concentrated simply by removing water. In this case, a membrane with the ability to reject small organic components and salts is required. Reverse osmosis membranes have been previously used for whey concentration [5,6].

Reverse osmosis utilises high applied hydraulic pressures to overcome the osmotic pressure of whey, resulting in high energy consumption for pumping [7] and the formation of a fouling layer on the membrane surface [8,9]. Recently, interest was shown in the use of forward osmosis for the concentration of whey, among other liquid foods [10–13]. Forward osmosis utilises the chemical potential gradient of a solvent (usually water) across a semi-permeable membrane. The solvent in the feed has a high chemical potential and moves to a draw solution on the other side of the membrane where its chemical potential is lower, until an osmotic equilibrium is established [14,15]. The draw solution is highly concentrated with an inorganic, organic or other solute and consequently has high osmotic pressure [16,17]. Intrinsically, the maximum osmotic pressure of the draw solution depends on the solubility of the solute.

Previous studies on the application of forward osmosis for whey concentration employed draw solution osmotic pressures of 90-100 bar [18–20], surpassing the hydraulic pressure equivalent employed in reverse osmosis, which typically lies in the range of 40 to 50 bar [7,21,22]. Considering this advantage of forward osmosis, whey samples of initially high osmotic pressure can be processed and concentrates of higher concentration factor can be potentially achieved. Previous bench scale studies on the concentration of whey using forward osmosis utilised NaCl and NH_4HCO_3/NH_4OH as the draw solution and resulted in whey total solids contents of 28 % and 21% [18,19]. However, the draw solution is diluted during the forward osmosis process and needs to be regenerated, which imposes an additional cost to the overall process [17].

Water permeate flux, J_w, in forward osmosis is proportional to the effective osmotic pressure difference across the active layer of the membrane, $\Delta\pi_{eff}$, and the water permeability coefficient of the membrane, A (Eq. 1). The effective osmotic pressure, $\Delta\pi_{eff}$, is the difference between the

osmotic pressure of the draw solution and feed at the surface of the active layer, $\pi_{D,m}$ and $\pi_{F,m}$, respectively (Eq. 2).

$$J_w = A\,\Delta\pi_{eff} \quad (1)$$

$$\Delta\pi_{eff} = \pi_{D,m} - \pi_{F,m} \quad (2)$$

These active layer surface osmotic pressures for the feed and draw solution are not equal to their corresponding bulk osmotic pressures, $\pi_{F,b}$ and $\pi_{D,b}$, due to concentration polarisation. Concentration polarisation results from a change in concentration of solute present in either the feed or the draw solution close to the active layer surface. For an asymmetric FO membrane where the feed faces the active layer and the draw solution faces the support layer, external concentration polarisation (ECP) and internal concentration polarisation (ICP) are evident on the active layer and within the support layer, respectively (Fig. 1) [23].

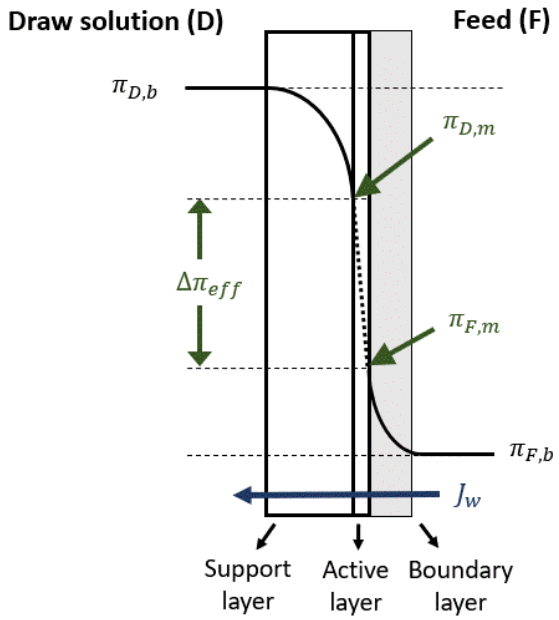

Fig. 1 Effective osmotic pressure driving force, $\Delta\pi_{,eff}$, for a forward osmosis membrane subject to concentrative external concentration polarisation (ECP) on the feed (F) side ($\pi_{F,m} > \pi_{F,b}$) and dilutive internal concentration polarisation (ICP) on the draw solution (D) side ($\pi_{D,m} < \pi_{D,b}$).

ECP is concentrative for the feed due to the formation of a boundary layer close to the active layer, which poses a resistance to the diffusion of solute back into the bulk solution. Thus, the effective osmotic pressure, $\pi_{F,m}$, is expected to be higher than the bulk, $\pi_{F,b}$. ICP is dilutive for the draw solution, implying that $\pi_{D,m}$ is lower than $\pi_{D,b}$, because as the draw solute diffuses through the support layer it encounters a resistance inherent of the structure of the support layer and is diluted by the water permeating across the membrane. A model has been developed to predict water permeate flux for an FO membrane which takes into account both concentrative ECP and dilutive ICP

gradients. These gradients are dependent on the mass transfer coefficient on the feed side of the membrane, k, and the resistance to draw solute diffusion across the support layer, K (Eq. 3). This implicit flux model requires knowledge of the feed channel dimensions to determine k, the membrane support layer characteristics to determine K, and the feed and draw solution osmotic pressures.

$$J_w = A\left[\pi_{D,b}\exp(-J_w K) - \pi_{F,b}\exp\left(\frac{J_w}{k}\right)\right] \quad (3)$$

An estimate of k can be obtained from calculation of the dimensionless Sherwood number, Sh, (Eq. 4) by applying appropriate correlations involving the Reynolds number, Re, and Schmidt number, Sc (Eq. 5) where d_h is the hydraulic diameter of the channel, L is the channel length and D is diffusion coefficient of the draw solute across the membrane [24,25]. This determination may be a challenging task for a commercial spiral-wound configuration membrane fitted with feed spacers. Moreover, the mass transfer coefficient varies dynamically during the concentration process, due to changes in the feed density, viscosity and concentration of dissolved compounds. Solute resistivity, K, was previously defined for a forward osmosis process by Eq. 6, where B is the permeability coefficient of the draw solute [26,27]. The value of K for cellulose triacetate (CTA) bench scale flat-sheet forward osmosis membranes has been previously calculated using this equation by assuming that the membrane has a high rejection of solute, thus B approaches zero [23,27]. In turn, the solute resistivity depends on the structure of the support layer, expressed as the structural parameter, S, and the draw solute used (Eq. 7). Flat-sheet CTA membranes characterised in previous studies were shown to have structural parameters in the range of 480 to 540 µm [28,29]. The calculation can be further simplified if a solution of negligible osmotic pressure is used as the feed.

$$k = \frac{Sh\,D}{d_h} \quad (4)$$

$$Sh = a\,Re^b\,Sc^c\left(\frac{d_h}{L}\right)^d \quad (5)$$

$$K = \left(\frac{1}{J_w}\right)\ln\left(\frac{B + A\,\pi_{D,b}}{B + J_w + A\,\pi_{F,m}}\right) \quad (6)$$

$$K = \frac{S}{D} \quad (7)$$

Information on the concentration of whey at pilot scale using FO is limited [13]. In most reported forward osmosis studies, the osmotic pressure driving force is given in terms of the bulk whey and draw solution osmotic pressures, and not the effective osmotic pressure at the membrane surface. Moreover, the effect of the osmotic pressure of whey as it is concentrated on permeate flux was not discussed. In an industrial environment, an in-situ assessment of the effective osmotic pressure driving

force without external measurements can be useful. Considering the above, the present work aims to assess the performance of a pilot scale forward osmosis filtration system for the concentration of cheese whey and provide a short-cut approach to quantify the effective osmotic pressures of the feed and draw solution throughout the concentration process. This simple method requires no external measurements of feed osmotic pressure and no information regarding the hydrodynamics of the spiral-wound membrane module. This short-cut method can be adopted to other, complex feed streams to be treated by forward osmosis.

2 Experimental

2.1 Materials

2.1.1 Whey specification

Liquid whey produced during the manufacture of blue cheese from pasteurised milk was supplied by High Weald Dairy, West Sussex, at a pH of 4.8 ± 0.2, conductivity of 6.9 ± 0.1 mS/cm and total solids (TS) content of 6.6 ± 0.5 %. The detailed composition of the inorganic constituents and the solids content of the initial whey (I) and the concentrate (C) are provided in Table 1.

Table 1: Composition of blue cheese whey samples used in the pilot scale forward osmosis process; Elemental analysis (ICP-OES) and solids content, expressed as total solids, ash and organics percentage. The estimated concentration factor of each constituent is expressed as the ratio of the concentrate to the initial whey (C/I) on a 'wet' basis of liquid sample. The ratio (C/I) was also calculated on a 'dry' basis (g /100g solids). Standard deviations of the inorganic constituents were obtained from triplicate measurement the sample. Standard deviations of total solids, ash and organic contents were obtained for duplicate measurement of the sample.

Property	**Sample 1 (I)**	**Sample 1 (C)**	**Ratio (C/I)**	**Ratio (C/I) – dry basis (g/100 g solids)**	**Sample 2 (I)**	**Sample 2 (C)**	**Ratio (C/I)**	**Ratio (C/I) – dry basis (g/100 g solids)**
Ca (mg/L)	451±1	1303±3	2.89±0.01	1.03	642±2	1756±3	2.74±0.01	1.02
K (mg/L)	1385±1	4321±15	3.12±0.01	1.11	1122±8	3526±6	3.14±0.02	1.15
Mg (mg/L)	84.9±1	235±2	2.77±0.04	0.98	118±1	323±1	2.73±0.02	1.02

Na (mg/L)	435±2	1498±9	3.44±0.03	1.22	597±1	1981±13	3.32±0.02	1.23
P (mg/L)	435±15	1165±10	2.68±0.1	0.95	709±4	1913±5	2.7±0.02	1.00
Total Solids (%)	6.3 ±0.02	17±0.04	2.69±0.01	-	7.1±0.02	18.3±0.05	2.58±0.01	-
Ash (%)	0.57±0.02	1.5±0.01	2.62±0.09	-	0.55 ± 0.03	1.6±0.01	2.89±0.15	-
Organics (%)	5.7±0.001	15.5±0.03	2.71±0.01	-	6.6± 0.01	16.6±0.04	2.51±0.01	-
Density (kg/L)	1.022	1.066	-	-	1.021	1.067	-	-

2.1.2 Draw solution

Food grade pure sodium chloride (NaCl) (Brenntag, UK) and tap water (water hardness of approximately 230 ppm expressed as $CaCO_3$) were used for the preparation of all draw solutions. Sodium chloride was selected as the draw solution for concentrating whey, as it has potential to be recycled within the cheese-making process. The initially highly concentrated solution is diluted as a result of the forward osmosis process. The concentration of the final solution can be corrected by addition of water or NaCl and further used in the salting or 'brining' process of certain types of cheese.

2.1.3 Membrane cleaning and maintenance

Chemical cleaning of the membrane was performed using citric acid, $C_6H_8O_7$ as well as an enzyme blend and neutral buffer in liquid form, as implemented in our previous study [13]. Sodium metabisulphite, $Na_2S_2O_5$, was used for membrane preservation at a concentration of 500 mg/L. All membrane cleaning and preservation agents were kindly provided by Holchem Laboratories Ltd.

2.1.4 Pilot forward osmosis filtration system

A pilot forward osmosis filtration plant was utilised, a detailed description of which is provided in our previous study [13]. The maximum volume capacity of the feed and draw solutions were approximately 250 L. The liquid circulation volume of the pilot plant, including the liquid filling the membrane module, pumps and piping was 34 L for the feed side and 11 L for the draw solution side. Depending on the filtration mode used, single-pass FO or batch FO, the initial volumes for the feed and draw solution were selected accordingly (see Sections 2.2.3 and 2.2.4). The circulation volume

was accounted for in the calculation of flux. At the beginning of all experiments, the volume of pre-existing water in the system was purged, in order to ensure that the circulation volume was filled with the feed and draw solution.

2.1.5 Membrane module

The FO membrane module comprises of two commercial spiral-wound CTA membranes elements (model FO-CTA-8040-45-SDS, Fluid Technology Solutions ($FTSH_2O$), Albany, USA), of a total active surface area of filtration, A_m, of 24 m^2. These membranes are fitted with medium feed spacers and standard draw solution spacers and are suitable for processing of moderate-fouling liquids such as skim milk. The membranes have a pH operating range from 3 to 7 and their maximum operating temperature is 60°C. The elements were assembled in series via an interconnector ($FTSH_2O$), within an 80" long pressure vessel (model ROPV R80B300S, Hydropure A/Asia Pty, Queensland, Australia). Custom end-caps (First Line Environment Technology, Harbin, China) were employed to seal and secure the membrane elements within the pressure vessel. The feed and draw solutions are in counter-current flow [13] to allow a higher osmotic pressure driving force along the entire length of the module [30]. A minimum transmembrane pressure of 0.35 bar (higher on the side ports of the module) is required in order to prevent element seam failure. The pressure applied on the side ports should not exceed 5 bar. The cross-flow velocity was estimated from the calculated area of cross-flow of the feed channel and the volumetric flow rate of the feed. A feed cross-flow velocity of 0.12 m/s was used in all the experiments.

2.2 Methods

2.2.1 Osmotic pressure of draw solution

The osmotic pressure of the draw solution was determined by measuring its water activity, α, at different concentrations of salt. Water activity was measured via a water activity probe (Rotronic Instruments) at 20 ± 2 °C. Osmotic pressure, π, was determined using Eq. 7, where V° is the molar volume of the solvent, T is the absolute temperature of solution and R is the universal gas constant [15,31]. The concentration of the NaCl was determined using a calibrated conductivity meter (Mettler Toledo, UK).

$$\pi = \left(-\frac{RT}{V^{\circ}}\right) \ln \alpha \quad (7)$$

2.2.2 Determination of pure water permeability coefficient (RO mode)

The pure water permeability coefficient of the membrane, A, was determined by measuring the water permeate flux, J_w, as a function of transmembrane hydraulic pressure, ΔP. Water at a temperature of 20 ± 2 °C was used on both the feed and draw solution sides. The average ΔP was maintained below

2.5 bar in order to comply with the low tolerance of the membrane module to hydraulic pressure. The flux was calculated using Eq. 8 (in L/m^{2}h), where ΔM is the change in mass of whey over a time interval, Δt, ρ is the density of whey and A_m is the effective membrane surface area.

$$J_w = \frac{\Delta M}{\rho\, A_m\, \Delta t} \quad (8)$$

2.2.3 Flux experiments with water as feed (single-pass FO mode)

Experiments were performed in forward osmosis (FO) mode, with the water as the feed and NaCl as the draw solution. Water was recirculated while the draw solution was continuously purged in a single-pass FO mode to maintain a constant bulk osmotic pressure, $\pi_{D,b}$. The initial volumes of the feed and the draw solution were 130 ± 2 L and 250 ± 2 L , respectively. To meet the minimum transmembrane pressure on the membrane module, the inlet pressure of the feed was set to 1.8 ± 0.1 bar and the draw solution inlet pressure was 0.55±0.05 bar, giving an average ΔP of approximately 1.1 bar. Flux was measured over a wide range of bulk draw solution osmotic pressures, while the osmotic pressure of water was considered negligible.

2.2.4 Batch flux experiments

2.2.4.1 Experiments with water as feed (batch FO mode)

Water and DS were re-circulated in batch FO mode. The initial volumes of the feed and the draw solution were 150 ± 2 L and 130 ± 2 L, respectively. As water permeated from the feed to the draw solution side, the volume of the feed decreased and the volume of the draw solution increased, thereby decreasing its osmotic pressure. Both the flux and the bulk draw solution osmotic pressure, $\pi_{D,b}$, were recorded as a function of time, until the amount water left in the feed tank was no longer enough for further pumping. Initial bulk draw solution osmotic pressures of 53, 64 and 75 bar were used. After each batch experiment the system was flushed with water on both the feed and draw solution sides until the conductivity of the purged water indicated no traces of NaCl had remained in the system.

2.2.4.2 Experiments with whey as feed (batch FO mode)

Batch permeate flux experiments using whey as feed were carried out at the same initial NaCl osmotic pressures, as well as feed and draw solution volumes described in Section 2.2.4.1. Two independent experiments were performed for each of the initial bulk draw solution osmotic pressures to assess the reproducibility of the results across different batches of whey. Samples of the whey were collected during the experiment, from which the total solids and percentage of inorganic material were determined according to the method described in our previous work [13]. Chemical cleaning was performed after each whey experiment.

3 Results and Discussion

3.1 Flux for water as feed

The water permeate flux was plotted as a function of net driving force when the system is operated in FO and RO modes (Fig. 2). Generally, the net pressure driving force is the maximum pressure driving force available for filtration, noted as $\left[\left(\pi_{D,b} - \pi_{F,b}\right) + \Delta P\right]$ (Eq. 3). In FO mode, this driving force was reduced to $\left(\pi_{D,b} + \Delta P\right)$ since water was used as feed, which has negligible osmotic pressure. In the RO mode where water was used in both the feed and draw solution sides, the net pressure driving force was taken simply as the average applied hydraulic pressure, ΔP. The plot of J_w as a function of ΔP showed the expected linear relationship (Eq. 1) where the gradient is the water permeability coefficient, A, which was evaluated as 0.484 L/m^{2}h bar. This value is in agreement with the 0.497 L/m^{2}h bar calculated for the same membrane module in our previous study [13]. Water permeability coefficients of 0.42-0.44 L/m^{2}h bar and 0.7 L/m^{2}h bar have also been reported for bench scale flat-sheet [28,32] and spiral-wound [33] CTA membranes at 20°C.

Data obtained for water and the draw solution in the single-pass and batch FO modes demonstrate that there is no difference in flux between the two modes (Fig. 2). However, flux in these FO modes does not increase linearly with the net driving force and has a lower value when compared to the RO mode for a given pressure driving force. This lower flux in the FO mode is caused by the internal concentration polarisation effect on the draw solution side of the membrane. This ICP effect is of dilutive nature because the direction of the water flux across the membrane causes the effective draw solution osmotic pressure, $\pi_{D,m}$, to be lower than $\pi_{D,b}$. The ICP gradient increases as $\pi_{D,b}$ increases, due to a higher flux. This result is in agreement with previous assessments of ICP in FO mode [23].

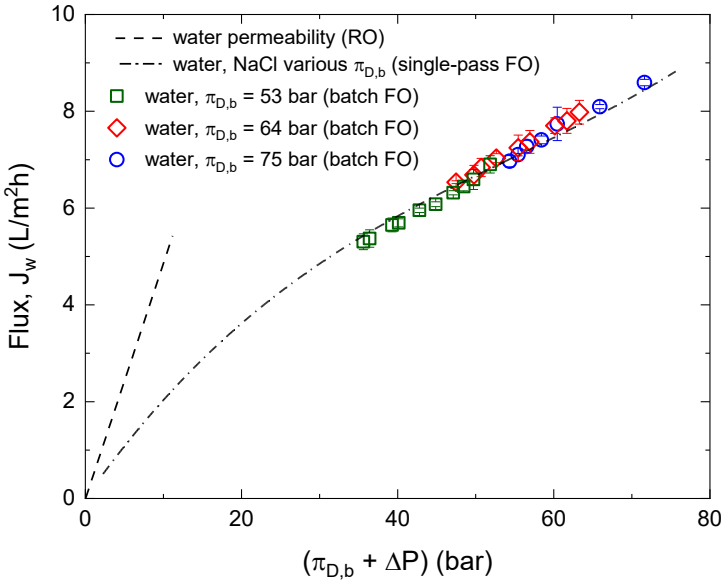

Fig. 2 Flux, J_w, as a function of net pressure driving force $\left[\left(\pi_{D,b} - \pi_{F,b}\right) + \Delta P\right]$ for water on both the feed and draw solution sides ($\pi_{D,b}, \pi_{F,b} = 0$) and the hydraulic transmembrane pressure, ΔP, is varied in the RO mode; water as feed and NaCl as the draw solution($\pi_{F,b} = 0,\ \Delta P = 1.1$ bar) and $\pi_{D,b}$ is varied in single-pass or batch FO mode.

3.2 Flux in whey batch experiments

For the whey experiments in the batch FO mode, the flux was recorded as a function of time for the three different initial bulk draw solution osmotic pressures (Fig. 3a). The initial flux was shown to increase from 4.2 ± 0.2 L/m^{2}h to 7.6 ± 0.5 L/m^{2}h, by increasing the initial bulk draw solution osmotic pressure from 53 bar to 75 bar. Flux decreased with time due to the gradual decrease in the osmotic of the draw solution caused by the water permeate and the gradual increase in the osmotic pressure of the whey as it became more concentrated. The flux was further plotted as a function of $\left(\pi_{D,b} + \Delta P\right)$, rather than the complete net pressure driving force $\left[\left(\pi_{D,b} - \pi_{F,b}\right) + \Delta P\right]$, as the bulk osmotic pressure of the whey was not known (Fig. 3b). The flux curves obtained for whey were compared with the curve obtained with water as the feed in the single-pass FO mode (Fig. 2). For all three initial bulk draw solution osmotic pressures, the initial flux (at the highest values of $\left(\pi_{D,b} + \Delta P\right)$) decreased at a similar rate as that for the case when water was used in the feed but started at a lower value. This lower value reflects the initial osmotic pressure of the whey, $\pi_{F,b}$. As the draw solution was further diluted, the flux decreased sharply and non-linearly for all initial bulk draw solution osmotic pressures and appeared to approach zero even when there was still a substantial residual net pressure driving force in the system.

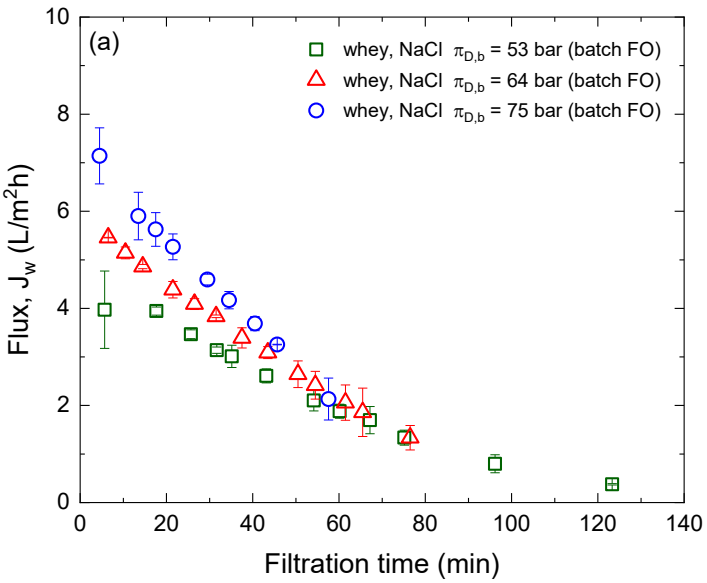

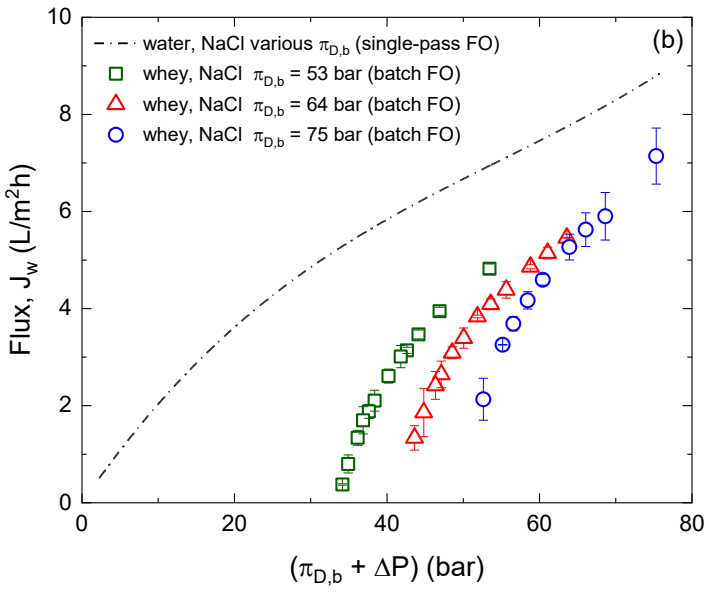

Fig. 3 Flux, J_w, of whey as a function of (a) filtration time and (b) bulk draw solution osmotic pressure and average transmembrane hydraulic pressure, $(\pi_{D,b} + \Delta P)$ for NaCl of initial bulk osmotic pressures of 53, 64 and 75 bar in the batch FO mode. Error bars represent deviations between two independent experiments. Dash-dotted line represents the flux curve for water as feed and NaCl draw solution in the single-pass FO mode.

The steeper decline in the whey flux compared to water as feed (Fig. 3b) is attributed to the increase in the bulk osmotic pressure of whey, $\pi_{F,b}$, as filtration progresses, as well as the development of (concentrative) external concentration polarisation on the feed side of the membrane. The apparent residual net pressure driving force when flux becomes zero, specifically represents the osmotic pressure of whey at the end of the filtration process, which is counter balancing the pressure driving force from the hydraulic and draw solution osmotic pressure $(\pi_{D,b} + \Delta P)$. At this point, the

concentration polarisation gradients approach zero, due to the negligible flux (Eq. 3), implying that the effective osmotic pressure of whey at the membrane surface, $\pi_{F,m}(t_f)$, becomes equal to the final bulk osmotic pressure of whey, $\pi_{F,b}(t_f)$. Extrapolation of the water permeate flux curves to zero indicates values of $\pi_{F,b}(t_f)$ of 34 bar, 45 bar and 50 bar for the initial bulk draw solution osmotic pressure of 53, 64 and 75 bar, respectively.

If a linear proportionality between the osmotic pressure and concentration of solutes in whey is assumed, the three extrapolated values of $\pi_{F,b}$ when flux is zero can be used to estimate the bulk osmotic pressure of whey throughout the filtration process, $\pi_{F,b}(t)$ (Eq. 9). This method was used for the experiments where the initial draw solution osmotic pressure was 53 bar. A similar flux extrapolation approach has been previously reported by Merson and Morgan [34], for estimating the osmotic pressure of juice solutions concentrated by reverse osmosis. The physical correctness of the method was later verified and used for the development of membrane osmometers [35,36].

$$\pi_{F,b}(t_n)V(t_n) = \pi_{F,b}(t_{n-1})V(t_{n-1}) \quad (9)$$

With the bulk whey osmotic pressure evaluated by Eq. 9, flux was replotted as a function of the corrected pressure driving force, $\left[\left(\pi_{D,b} - \pi_{F,b}\right) + \Delta P\right]$ (Fig. 4). The flux was now shown to vary linearly with pressure, indicating that the corrected pressure driving force is more representative of the effective driving force in the concentration of whey in the batch FO mode. Further, the curves for all three initial bulk draw solution osmotic pressures were shown to be concurrent. However, the gradients are much lower than that calculated for the pure water permeability in the RO mode (Fig. 2). At any value of flux, the difference between the pure water and whey curves is attributed to the effects of ICP on the draw solution side and ECP on the feed side of the membrane. This is true because for the pure water flux curve, the hydraulic transmembrane pressure represents the effective driving force, equivalent to an effective osmotic pressure difference in the FO mode.

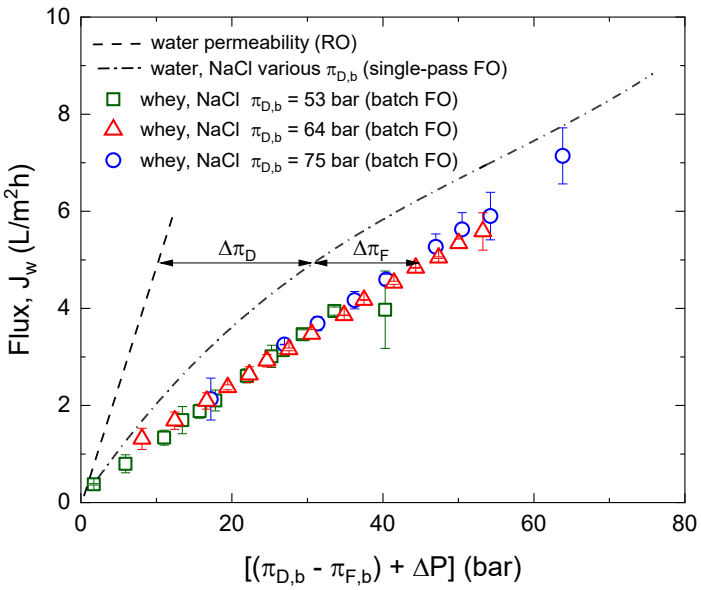

Fig. 4 Flux, J_w, of whey FO filtration as a function of the corrected bulk osmotic pressure and average hydraulic transmembrane pressure, $[(\pi_{D,b} - \pi_{F,b}) + \Delta P]$, for NaCl of initial bulk osmotic pressures of 53, 64 and 75 bar in the batch FO mode. Dashed line represents pure water flux in the RO mode. Dash-dotted line represents the flux curve for water as feed and NaCl draw solution in the single-pass FO mode.

3.3 Evaluation of effective osmotic pressure of whey and draw solution

The three flux curves obtained in Fig. 4 were used as the basis for implementing a short-cut methodology to evaluate the effective draw solution and feed osmotic pressures at the membrane surface. The two effective pressures, $\pi_{D,m}$ and $\pi_{F,m}$, were expressed as the sum of the bulk osmotic pressure and a pressure difference due to concentration polarisation effects. The concentration polarisation is dilutive for the draw solution, suggesting that $\pi_{D,m}$ is lower than $\pi_{D,b}$ by a pressure difference $\Delta\pi_D$ (Eq. 10). Respectively, concentration polarisation is concentrative for whey, implying that $\pi_{F,m}$ is higher than $\pi_{F,b}$ by a pressure difference $\Delta\pi_F$ (Eq. 11).

$$\pi_{D,m} = \pi_{D,b} - \Delta\pi_D \quad (10)$$

$$\pi_{F,m} = \pi_{F,b} + \Delta\pi_F \quad (11)$$

Each of the three curves in Fig. 4 was expressed by a flux equation, depending on the effective driving force; pure water in RO mode (Eq. 12), water-NaCl in single-pass FO mode (Eq. 13) and whey-NaCl (Eq. 13). Consequently, at any given value of flux, $\Delta\pi_D$ can be calculated from the difference between the water and water-NaCl curves (Eq. 12 and Eq. 13) and $\Delta\pi_F$ can be evaluated from the difference between the water-NaCl and whey-NaCl curves (Eq. 13 and Eq. 14). Substituting the values of $\Delta\pi_D$ or $\Delta\pi_F$ in Eq. 10 or Eq. 11, respectively, provides the corresponding effective osmotic pressure at the membrane surface, given that the bulk osmotic pressures are known experimentally.

$$J_w = A\,\Delta P \quad (12)$$

$$J_w = A\left[\left(\pi_{D,b} - \Delta\pi_D\right) + \Delta P\right] \quad (13)$$

$$J_w = A\left[\left(\pi_{D,b} - \Delta\pi_D\right) - \left(\pi_{F,b} + \Delta\pi_F\right) + \Delta P\right] \quad (14)$$

3.4 Verification of short-cut method based on FO model fitting

The short-cut method, as described in Section 3.3, was employed to evaluate the effective osmotic pressure of whey without the need of external osmotic pressure measurements. This is useful when complex solutions such as liquid foods are to be concentrated using forward osmosis and little is known of their composition or osmotic pressure. To verify the validity of this approach, experimental data were fitted to the implicit flux model (Eq. 3), by obtaining additional data and simplifying assumptions. This analysis was applied to the results from Sample 2 (Table 1), which was concentrated using an initial bulk draw solution osmotic pressure of 53 bar. The solute resistivity of the membrane support layer, K, was obtained from the batch FO experiments using water as the feed via Eq. 6, assuming a negligible osmotic pressure of the feed. The effect of the draw solute permeability coefficient, B, on flux was considered to be negligible, further simplifying Eq. 6, . The solute resistivity, K, was found to be equal to 0.089 m^2h/L (or 3.2 $\times 10^5$ m^2s/m^3). This value corresponds to a membrane structural parameter of 474 µm, which is in agreement with values previously reported for CTA membranes [28].

The bulk osmotic pressure of the draw solution, $\pi_{D,b}$ (as measured in the FO experiment), the graphically estimated bulk osmotic pressure of whey, $\pi_{F,b}$, the membrane water permeability coefficient A and the solute resistivity K, were substituted into Eq. 3. The modelled flux was forced to match the experimental value of flux, by using the mass transfer coefficient, k, as the fitting parameter. The resulting mass transfer coefficient ranged from to 5.8 to 9 L/m^2h (1.6×10^{-6} to 2.5×10^{-6} m/s). This variation in the mass transfer coefficient can be related to altered hydrodynamic conditions in the feed channel as whey becomes more concentrated. Evaluation of the mass transfer coefficient based on a correlation of the form given by Eq. 5 would require extensive characterisation of the density and viscosity of whey as a function of its concentration factor, parameters affecting the Reynolds and Schmidt numbers, Re and Sc, and consequently the Sherwood number, Sh.

With the mass transfer coefficient known, the effective osmotic pressure of the feed and draw solution were calculated from Eq. 3, and the resulting, $\pi_{F,m,flux}$ and $\pi_{D,m,flux}$ respectively, were compared to the effective osmotic pressures calculated through the short-cut approach, $\pi_{F,m,shortcut}$

and $\pi_{D,m,shortcut}$ (Fig. 5). The short-cut approach and the flux model produced similar results, verifying that the short-cut approach can be used for evaluating effective osmotic pressures in the batch FO mode. This simple method can easily be implemented to other liquid food systems with complex composition, where estimation of their osmotic pressure can be challenging or requires a number of different measurements. A necessary condition for applying the proposed method is to allow filtration to progress to the point where the flux approaches zero, implying that an osmotic equilibrium is attained. Under these conditions the final value of the osmotic pressure of whey can be obtained.

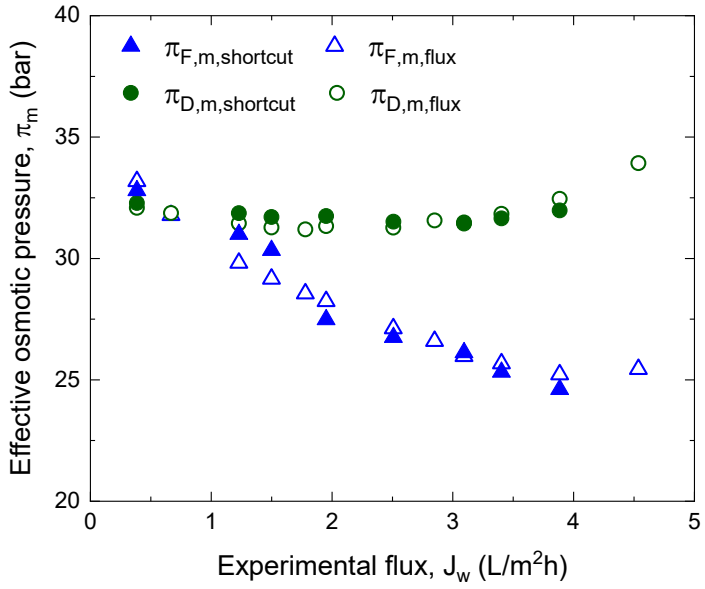

Fig. 5 Effective osmotic pressure as a function of the experimental flux for both draw solution and whey feed, as demonstrated for whey sample 2 using short-cut approach ($\pi_{F,m,shortcut}$ and $\pi_{D,m,shortcut}$) and compared to the forward osmosis flux model ($\pi_{F,m,flux}$ and $\pi_{D,m,flux}$). Whey was concentrated in the batch FO mode using NaCl draw solution of an initial bulk osmotic pressure of 53 bar.

3.5 Osmotic pressure of whey and concentration factor

This study demonstrates a simple method for empirically quantifying the osmotic pressure of whey throughout the batch forward osmosis concentration process. The effective osmotic pressure of whey as determined using the short-cut approach, $\pi_{F,m,shortcut}$ was plotted as a function of concentration factor of whey and compared to the bulk osmotic pressure of whey as determined graphically from the experimental flux curves, $\pi_{F,b}$ (Fig. 6). At a low concentration factor, corresponding to the initial stages of the batch process where flux is high, the difference between $\pi_{F,m,shortcut}$ and $\pi_{F,b}$ is high. This demonstrates a high concentration polarisation effect, which is in agreement with the theoretical flux model (Eq. 3). As filtration progresses flux decreases, due to an increase in $\pi_{F,b}$ (and decrease in $\pi_{D,b}$), causing the difference between $\pi_{F,m,shortcut}$ and $\pi_{F,b}$ to become gradually smaller. As flux

approaches zero, the two pressures attain the same value, corresponding to the maximum osmotic pressure of whey during the filtration process.

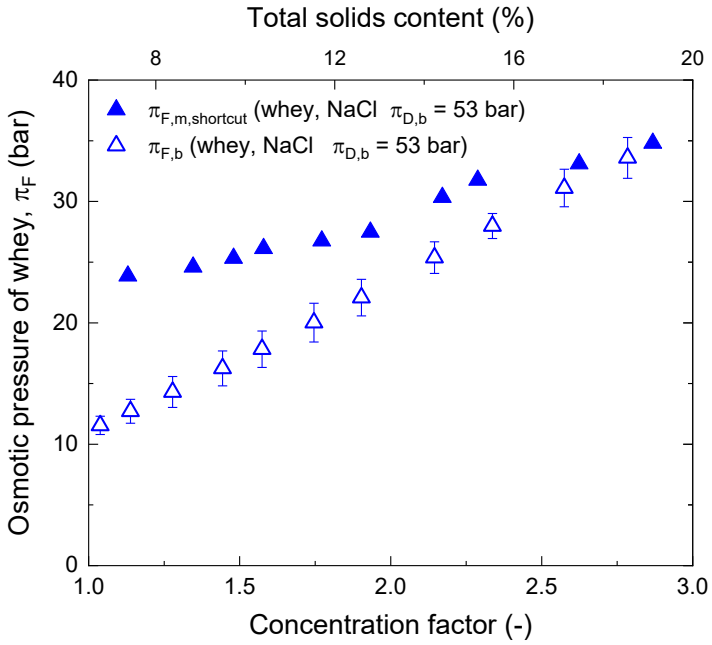

Fig. 6 Effective osmotic pressure of whey, $\pi_{F,m,shortcut}$ (obtained using the short-cut approach), and bulk osmotic pressure of whey, $\pi_{F,b}$ (obtained graphically from experimental data), as a function of whey concentration factor, for the experiments in the batch FO mode using NaCl draw solution of an initial bulk osmotic pressure of 53 bar.

The maximum concentration factor of whey achieved in the pilot scale forward osmosis concentration process was 2.7 ± 0.1, or 17 ± 1 % in terms of total solids, for all the initial bulk draw solution osmotic pressures used. For the lower initial osmotic pressure of NaCl of 53 bar, osmotic equilibrium was approached. However, the experiments at higher initial NaCl osmotic pressures of 64 and 75 bar clearly demonstrated that a higher concentration factor would have been achieved, if the filtration system was able to further process the small amount of whey towards the end of the process. This suggests that in order to achieve a higher concentration factor in an industrial filtration system, a 'feed and bleed' filtration mode would be suitable, which is commonly used in industry [37,38]. Another limiting factor for concentration, in addition to osmotic pressure, would be the increasing viscosity of whey, which dictates the ability of the concentrate produced to flow through the membrane filtration system. Based on previous work done on milk, flow no longer occurs after a concentration factor of 40-50% of solids is reached [2,39]. In addition, at a total solids content of approximately 40%, spontaneous lactose crystallisation may occur [2].

The ratios of the individual inorganic elements in the initial whey and concentrate (Table 1) were found to be slightly higher than that of the total solids for both whey samples 1 and 2. Clearly the ratio is higher for sodium (Na) compared to the other elements for both samples. This can be attributed to the reverse diffusion of sodium from the draw solute into whey throughout the duration of the concentration process in the batch FO mode. This addition of sodium is unlikely to cause any concerns on product quality, as discussed in our previous study [13]. The slightly higher ratios for potassium, calcium and magnesium may be within experimental error, as demonstrated by the ratio of concentrate to initial sample, C/I, calculated on a dry basis (g of inorganics/100g of solids). Alternatively, they may reflect a loss of some organic content to the draw solution lowering the ratio for these solutes. The transport of organic constituents of whey to the draw solution was discussed in detail in our previous study [13]. It was found that small organic compounds such as lactose and peptides were transferred from the bulk skim milk or whey, resulting in a foaming effect on the draw solution. A loss of organic constituents, which are significantly higher relative to the inorganic constituents has probably been minimal in the present study, as the ratio C/I for the organics is essentially the same as that of the total solids.

3.6 Suitability of the method to other feed streams and limitations

The short-cut method developed here was proven accurate in evaluating the effective osmotic pressure of a relatively complex feed such as cheese whey. Whey represents a feed with substantial amounts of suspended and soluble matter. Various other complex liquids in the food and dairy industry often require concentration, including fruit juices, skim milk or lactose solutions [4,40–42]. This method can be directly utilised to other liquid streams concentrated using a batch forward osmosis process and enables to evaluate the effective osmotic pressure driving force, without the need to evaluate the osmotic pressure of the feed in advance.

Both the proposed method and the forward osmosis model only account for the presence of concentration polarisation but do not account for the occurrence of fouling. In the present work, the experimental data have not indicated the presence of fouling in the system. The flux obtained for whey matched that when synthetic NaCl solutions were used as the feed which were concentrated in the batch FO mode using initial draw solutions osmotic pressures of 53 and 75 bar (Fig. A1, Appendix A). In the presence of fouling, the experimental flux for a given pressure driving force would deviate from that predicted by the forward osmosis model. Moreover, the method as developed in the present study assumes a decreasing bulk osmotic pressure of the draw solution due to the batch FO mode. The proposed short-cut method cannot be directly extrapolated to a continuous process where the draw solution is constantly regenerated in order to maintain a constant bulk osmotic pressure.

4 Conclusions

The present work demonstrates the potential of forward osmosis for the concentration of cheese whey in a pilot filtration system operated in a batch mode. The process produced concentrates with a concentration factor of approximately 2.7, by increasing the total solids content of whey from 6.5 to 18%. The maximum initial permeate flux was 7.2 L/m^{2}h, obtained for an initial draw solution osmotic pressure of 74 bar. The bulk osmotic pressure of whey was determined graphically from the permeate flux curves plotted as a function of the bulk draw solution osmotic pressure and hydraulic pressure, as the osmotic pressure of whey was initially unknown. The bulk osmotic pressure of whey was shown to increase from 12 to 34 bar over the course of the batch forward osmosis process. It was also shown that the final whey osmotic pressure can exceed osmotic pressures encountered in previous reverse osmosis studies. Based on the theoretically known effective pressure driving force, obtained from the pure water permeability of the membrane, the effective feed and draw solution osmotic pressures were evaluated via a new short-cut approach. The short-cut approach was verified based on first principles, by applying the forward osmosis flux model to the experimental data.

The study provides important information regarding flux performance at pilot scale, while quantifying the effective osmotic pressures of the feed and draw solution. The proposed method requires no information in advance of the osmotic pressure of the feed and can be directly applied to the batch forward osmosis concentration of other complex liquid streams .The method is applicable only when the system is allowed to approach an osmotic equilibrium and where no fouling is encountered.

Acknowledgements

The authors would like to thank High Weald Dairy (West Sussex, UK) for kindly providing the whey for this work, as well as Holchem Laboratories Ltd (Bury, UK) for providing the membrane cleaning and preservation agents. Anna Artemi acknowledges the assistance of Oliver P. Crossley in carrying out the ICP-OES analysis.

References

[1] C. V Morr, E.Y.W. Ha, Whey protein concentrates and isolates: processing and functional properties, Crit. Rev. Food Sci. Nutr. 33 (1993) 431–476.

[2] G. Bylund, Whey Processing, Dairy Processing Handbook, in: Tetra Pak Dairy Process. Handb., 2019.

[3] E. Tsakali, K. Petrotos, A. D'Allessandro, P. Goulas, A review on whey composition and the methods used for its utilization for food and pharmaceutical products, in: Proc. 6th Int. Conf. Simul. Model. Food Bioind., 2010: pp. 195–201.

[4] G.Q. Chen, T.S.H. Leong, S.E. Kentish, M. Ashokkumar, G.J.O. Martin, Membrane Separations in the Dairy Industry, in: Sep. Funct. Mol. Food by Membr. Technol., Elsevier, 2019: pp. 267–304.

[5] E. Suárez, F. San Martín, R. Alvarez, J. Coca, Reverse osmosis of whey. Determination of mass transfer coefficients, J. Memb. Sci. 68 (1992) 301–305.

[6] M. Rosenberg, Current and future applications for membrane processes in the dairy industry, Trends Food Sci. Technol. 6 (1995) 12–19.

[7] J.K. Donnelly, A.C. O'Sullivan, R.A.M. Delaney, Reverse smosis - concentration applications, Int. J. Dairy Technol. 27 (1974) 128–140.

[8] A.J.B. van Boxtel, Z.E.H. Otten, H.J.L.J. van der Linden, Evaluation of process models for fouling control of reverse osmosis of cheese whey, J. Memb. Sci. 58 (1991) 89–111.

[9] S.S. Madaeni, Y. Mansourpanah, Chemical cleaning of reverse osmosis membranes fouled by whey, Desalination. 161 (2004) 13–24.

[10] N.S. Terefe, F. Janakievski, O. Glagovskaia, K. De Silva, M. Horne, R. Stockmann, Forward osmosis: A novel membrane separation technology of relevance to food and related industries, Innov. Food Process. Technol. (2016) 177–205.

[11] K.B. Petrotos, H.N. Lazarides, Osmotic concentration of liquid foods, J. Food Eng. 49 (2001) 201–206.

[12] B. Jiao, A. Cassano, E. Drioli, Recent advances on membrane processes for the concentration of fruit juices: a review, J. Food Eng. 63 (2004) 303–324.

[13] G.Q. Chen, A. Artemi, J. Lee, S.L. Gras, S.E. Kentish, A pilot scale study on the concentration of

483 milk and whey by forward osmosis, Sep. Purif. Technol. (2019).

484 [14] J.G. Wijmans, R.W. Baker, The solution-diffusion model: a review, J. Memb. Sci. 107 (1995) 1–
485 21.

486 [15] R.W. Baker, Membrane technology and applications, Membr. Technol. (2004).

487 [16] Q. Ge, M. Ling, T.-S. Chung, Draw solutions for forward osmosis processes: developments,
488 challenges, and prospects for the future, J. Memb. Sci. 442 (2013) 225–237.

489 [17] A. Achilli, T.Y. Cath, A.E. Childress, Selection of inorganic-based draw solutions for forward
490 osmosis applications, J. Memb. Sci. 364 (2010) 233–241.

491 [18] C. Aydiner, U. Sen, S. Topcu, D. Sesli, D. Ekinci, A.D. Altınay, B. Ozbey, D.Y. Koseoglu-Imer, B.
492 Keskinler, Techno-economic investigation of water recovery and whey powder production
493 from whey using UF/RO and FO/RO integrated membrane systems, Desalin. Water Treat. 52
494 (2014) 123–133.

495 [19] C. Aydiner, U. Sen, S. Topcu, D. Ekinci, A.D. Altinay, D.Y. Koseoglu-Imer, B. Keskinler, Techno-
496 economic viability of innovative membrane systems in water and mass recovery from dairy
497 wastewater, J. Memb. Sci. 458 (2014) 66–75.

498 [20] C. Aydiner, S. Topcu, C. Tortop, F. Kuvvet, D. Ekinci, N. Dizge, B. Keskinler, A novel
499 implementation of water recovery from whey:“forward–reverse osmosis” integrated
500 membrane system, Desalin. Water Treat. 51 (2013) 786–799.

501 [21] D. Pepper, A.C.J. Orchard, Improvements in the concentration of whey and milk by reverse
502 osmosis, Int. J. Dairy Technol. 35 (1982) 49–53.

503 [22] J. Hiddink, R. de Boer, P.F.C. Nooy, Reverse Osmosis of Dairy Liquids, J. Dairy Sci. 63 (1980) 204–
504 214.

505 [23] J.R. McCutcheon, M. Elimelech, Modeling water flux in forward osmosis: implications for
506 improved membrane design, AIChE J. 53 (2007) 1736–1744.

507 [24] J. Mulder, Basic principles of membrane technology, 2012.

508 [25] J.R. McCutcheon, R.L. McGinnis, M. Elimelech, Desalination by ammonia–carbon dioxide
509 forward osmosis: influence of draw and feed solution concentrations on process performance,
510 J. Memb. Sci. 278 (2006) 114–123.

511 [26] S. Loeb, L. Titelman, E. Korngold, J. Freiman, Effect of porous support fabric on osmosis through

512 a Loeb-Sourirajan type asymmetric membrane, J. Memb. Sci. 129 (1997) 243–249.

513 [27] J.R. McCutcheon, M. Elimelech, Influence of concentrative and dilutive internal concentration
514 polarization on flux behavior in forward osmosis, J. Memb. Sci. 284 (2006) 237–247.

515 [28] W.A. Phillip, J.S. Yong, M. Elimelech, Reverse draw solute permeation in forward osmosis:
516 modeling and experiments, Environ. Sci. Technol. 44 (2010) 5170–5176.

517 [29] A. Tiraferri, N.Y. Yip, A.P. Straub, S.R.-V. Castrillon, M. Elimelech, A method for the
518 simultaneous determination of transport and structural parameters of forward osmosis
519 membranes, J. Memb. Sci. 444 (2013) 523–538.

520 [30] S. Mondal, R.W. Field, J.J. Wu, Novel approach for sizing forward osmosis membrane systems,
521 J. Memb. Sci. 541 (2017) 321–328.

522 [31] V.T. Granik, B.R. Smith, S.C. Lee, M. Ferrari, Osmotic pressures for binary solutions of non-
523 electrolytes, Biomed. Microdevices. 4 (2002) 309–321.

524 [32] M. Xie, W.E. Price, L.D. Nghiem, M. Elimelech, Effects of feed and draw solution temperature
525 and transmembrane temperature difference on the rejection of trace organic contaminants by
526 forward osmosis, J. Memb. Sci. 438 (2013) 57–64.

527 [33] Z. Wang, J. Zheng, J. Tang, X. Wang, Z. Wu, A pilot-scale forward osmosis membrane system for
528 concentrating low-strength municipal wastewater: performance and implications, Sci. Rep. 6
529 (2016) 21653.

530 [34] R.L. Merson, J.A. Morgan, Juice concentration by reverse osmosis, Food Technol. 22 (1968) 97–
531 100.

532 [35] H. Nabetani, M. Nakajima, Development of a new type of membrane osmometer, J. Chem. Eng.
533 Japan. 25 (1992) 269–274.

534 [36] A. Grattoni, G. Canavese, F.M. Montevecchi, M. Ferrari, Fast membrane osmometer as
535 alternative to freezing point and vapor pressure osmometry, Anal. Chem. 80 (2008) 2617–
536 2622.

537 [37] M. Dresch, G. Daufin, B. Chaufer, Integrated membrane regeneration process for dairy
538 cleaning-in-place, Sep. Purif. Technol. 22–23 (2001) 181–191. doi:10.1016/S1383-
539 5866(00)00128-3.

540 [38] S.E. Kentish, G. Rice, Demineralization of dairy streams and dairy mineral recovery using
541 nanofiltration, in: Membr. Process. Dairy Ingred. Sep., John Wiley & Sons, Ltd, Chichester, UK,

2015: pp. 112–138. doi:10.1002/9781118590331.ch5.

[39] I. Roy, A. Bhushani, C. Anandharamakrishnan, Techniques for the Preconcentration of Milk, in: Handb. Dry. Dairy Prod., John Wiley & Sons, Chichester, UK, 2017: pp. 23–41.

[40] G.Q. Chen, S.L. Gras, S.E. Kentish, The application of forward osmosis to dairy processing, Sep. Purif. Technol. 246 (2020) 116900.

[41] N.K. Rastogi, Applications of forward osmosis process in food processing and future implications, in: Curr. Trends Futur. Dev. Membr., Elsevier, 2020: pp. 113–138. doi:10.1016/b978-0-12-816777-9.00005-8.

[42] K. Belafi-Bako, I. Petrinić, C. Hélix-Nielsen, G. Sun, Y.W. Siew, S. Alvisse, N.X. Tung, A. Boor, N. Nemestothy, Osmotic driven membrane processes for separation of special food compounds, in: Sep. Funct. Mol. Food by Membr. Technol., Elsevier, 2018: pp. 383–401. doi:10.1016/B978-0-12-815056-6.00011-5.

Appendix A: Comparison of whey flux with a synthetic feed solution

Concentration experiments in the batch FO mode were also performed utilising NaCl as the feed, for the initial draw solution osmotic pressures of 53 and 75 bar. The initial osmotic pressure of these synthetic feed solutions was calculated to be 13 and 14 bar and was found to be slightly higher compared to the initial bulk osmotic pressure of whey, approximately equal to 11-12 bar (Fig. 6). The flux obtained for the two synthetic solutions is in good agreement with the flux obtained for whey (Fig. A1). These results indicate that no significant fouling has occurred over the range of total solids reported in the present study and that viscosity changes are minimal.

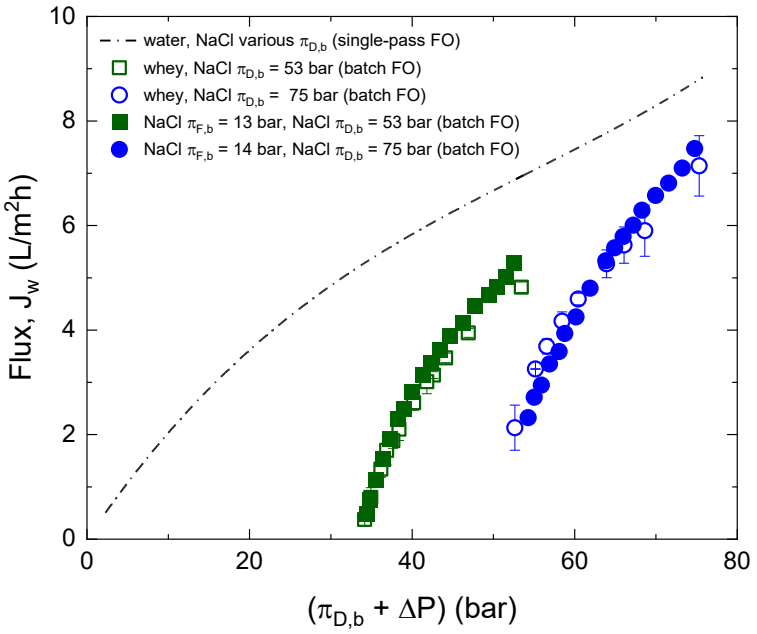

Fig A1. Flux, J_w, in FO filtration as a function of the osmotic pressure in the bulk of the draw solution and the average transmembrane hydraulic pressure, $(\pi_{D,b} + \Delta P)$. Feed solutions: synthetic NaCl solutions (initial bulk feed solution osmotic pressures, $\pi_{F,b}$, of 13 and 14 bar) and whey; Draw solutions: NaCl solutions with initial osmotic pressures, $\pi_{D,b}$, of 53 and 75 bar. The dashed line represents the flux curve for water as feed and NaCl as draw solution.